

Establishing a theory for deuteron-induced surrogate reactions

G. Potel,^{1,2} F. M. Nunes,^{1,3} and I. J. Thompson²

¹National Superconducting Cyclotron Laboratory, Michigan State University, East Lansing, Michigan 48824, USA

²Lawrence Livermore National Laboratory L-414, Livermore, California 94551, USA

³Department of Physics and Astronomy, Michigan State University, East Lansing, Michigan 48824-1321, USA

(Received 7 July 2015; published 18 September 2015)

Background: Deuteron-induced reactions serve as surrogates for neutron capture into compound states. Although these reactions are of great applicability, no theoretical efforts have been invested in this direction over the last decade.

Purpose: The goal of this work is to establish on firm grounds a theory for deuteron-induced neutron-capture reactions. This includes formulating elastic and inelastic breakup in a consistent manner.

Method: We describe this process both in post- and prior-form distorted wave Born approximation following previous works and discuss the differences in the formulation. While the convergence issues arising in the post formulation can be overcome in the prior formulation, in this case one still needs to take into account additional terms due to nonorthogonality.

Results: We apply our method to the $^{93}\text{Nb}(d,p)X$ at $E_d = 15$ and 25 MeV and are able to obtain a good description of the data. We look at the various partial wave contributions, as well as elastic versus inelastic contributions. We also connect our formulation with transfer to neutron bound states.

Conclusions: Our calculations demonstrate that the nonorthogonality term arising in the prior formulation is significant and is at the heart of the long-standing controversy between the post and the prior formulations of the theory. We also show that the cross sections for these reactions are angular-momentum dependent and therefore the commonly used Weisskopf limit is inadequate. Finally, we make important predictions for the relative contributions of elastic breakup and nonelastic breakup and call for elastic-breakup measurements to further constrain our model.

DOI: [10.1103/PhysRevC.92.034611](https://doi.org/10.1103/PhysRevC.92.034611)

PACS number(s): 21.10.Pc, 24.10.Eq, 24.10.Ht, 25.45.Hi

I. INTRODUCTION

Neutron-capture reactions $A(n,\gamma)B$ are very important in astrophysics for the production of heavy elements but are equally relevant in stewardship science, since it is through neutron capture that fission is induced and chain reactions begin. Most often, for low-energy neutrons, the capture proceeds through continuum states, forming a compound nucleus ($A + n \rightarrow B^*$) that then decays, either through γ emission to the ground state, or through other particle channels. The direct measurement of neutron capture is challenging, particularly because most of the targets of interest have short half-lives and neutrons cannot be made into targets. A proposed alternative it to use deuterons as surrogates [1]. In this indirect method, the proton inside the deuteron behaves mostly as a spectator, the neutron inside the deuteron is delivered to the target surface and gets absorbed by the target $A(d,p)B^*$. Since this is a compound-nucleus reaction, the final compound nucleus decays in the same way as after $A + n \rightarrow B^*$. An example of a recent measurement applying the surrogate method is the $^{171,173}\text{Yb}(d,p\gamma)$ experiment performed at LBNL [2]. The measurement was performed on a nucleus for which neutron-capture cross sections were already available. The neutron-capture cross sections extracted in the deuteron-induced reactions were in fair agreement with those measured directly.

While the exclusive process $A(d,pn)A$ (with A left in its ground state) is clearly identified as elastic breakup, the rest of the cross section arising from the inclusive process $A(d,p)X$,

where only the proton is measured in the final state, is harder to name because it encompasses many different processes. Some refer to this component of the cross section as inelastic breakup, breakup fusion, or partial fusion. In this work, we will always use the term “nonelastic breakup.”

Although there are important applications of the surrogate method for neutron capture, no theoretical development has taken place in the last two decades to establish the method on firm grounds. In terms of direct-reaction mechanisms, this process can be seen as inelastic breakup followed by fusion, or neutron transfer to the continuum. Significant theoretical effort took place in the eighties with the main idea being first introduced by Kerman and McVoy [3], with the works of Udagawa and Tamura [4] and Austern and Vincent [5] appearing shortly after. In Ref. [4] the authors assume the process $A(d,p)B^*$ is a two-step process: first breakup of the deuteron followed by fusion of the neutron. They describe this in distorted-wave Born approximation in prior form and make a number of additional approximations (we will denote this theory as “UT”). In Ref. [5], the starting point is the post-form distorted-wave Born approximation, and the authors assume that the target gets excited only by the neutron-target interaction (we will denote this theory as “AV”). One difficulty in this method is the convergence of the matrix element. In both Refs. [5] and [4], all (d,p) transfer cross sections to the excited states are summed without explicitly introducing the properties of these states. This is of course a key aspect in describing inclusive processes. As it turned out, cross sections obtained with the post (AV) theory did not agree

with those obtained with the prior (UT) theory. This generated a heated controversy that lasted a decade and was never fully resolved.

A detailed analysis of the UT theory is presented in Ref. [6], where several approximations are considered including the zero-range approximation and the surface approximation. The authors of Refs. [6,7] argue that the theory of AV includes unphysical components which should be corrected by inclusion of a nonorthogonality term. On the other hand, Ichimura *et al.* [8] in their detailed examination conclude that certain implicit approximations made in the optical reductions by UT are at the heart of the disagreement. Although several groups revisited the matter later [9–12], establishing a relationship between the various theories, the controversy on the relevance of the nonorthogonality term was never resolved. Nowadays, many of the approximations made in the early eighties have become unnecessary, and thus it makes sense to revisit the issue.

Two recent works have applied the AV theory to study a variety of reactions [13,14]. In Lei and Moro [13] these reactions include deuteron breakup on ^{58}Ni at intermediate energies, deuteron breakup on ^{93}Nb at lower energies, and ^6Li elastic scattering on ^{209}Bi around the Coulomb barrier. In order to deal with the convergence of the amplitude, the authors of Ref. [13] construct continuum bins corresponding to a square integrable wave packet obtained by averaging the scattering states over energy. These studies [13,14] show that, overall, the AV theory provides a good description of the processes considered.

Given the recent experimental interest in the surrogate method, it is critical to develop a theory that is practical and reliable. Our overall goal with this work is exactly to establish such a theory, which can then serve as a starting point to make further improvements in the future. In this work we present our own derivations of the elastic- and inelastic-breakup amplitudes in both the post (AV) and prior (UT) forms, within the distorted-wave Born approximation (Sec. II). We show that these two theories are indeed equivalent if no further approximations are made, although the post formalism introduces numerical difficulties which are avoidable by the prior formalism. We also show that a nonorthogonality term and additional cross terms naturally arise in the UT theory. This is a consequence of the fact that, when writing the amplitude in the prior form, no easy separation between the breakup process and the excitation process is possible. In other words, in the prior formalism, breakup and excitation are entangled. These days, however, their computation poses no difficulty. Following the work of Ref. [15], in Sec. II C, we use the same framework to study neutron transfer to bound states. This establishes an important connection between scattering and bound states and provides a stringent test for the theory. We apply the method to surrogate reactions of deuterons on ^{93}Nb for beam energies in the range of 10 to 20 MeV to compare with data, as done by Ref. [16] (Sec. III). We analyze our results and dissect the various contributions in terms of angular momentum, as well as the relative magnitude of elastic versus nonelastic cross sections. Finally, in Sec. IV, we draw our conclusions and provide an outlook into further possible developments.

II. THEORETICAL FORMULATION

A. General formalism in the *post* representation (AV)

Let us consider the reaction $A(d,p)B^*$ which includes elastic breakup and any other inelastic processes. In this section, we follow closely the work by Austern *et al.* [5] and derive the post-form amplitude for the process. We adopt a spectator approximation for the proton, which means the proton-target interaction will not explicitly excite the target A . We thus start by substituting the proton-target interaction $V_{Ap}(r_{Ap}, \xi_A)$ by an optical potential $U_{Ap}(r_{Ap})$. In addition, for the purpose of our derivation, we consider A to be infinitely massive. However, in the actual numerical applications, the recoil of the nucleus A is fully taken into account.

The three-body Hamiltonian for the problem is

$$H = K_n + K_p + h_A(\xi_A) + V_{pn}(r_{pn}) + V_{An}(r_{An}, \xi_A) + U_{Ap}(r_{Ap}), \quad (1)$$

where K_n and K_p are the kinetic-energy operators acting on the neutron and proton coordinates, respectively. We now consider the model wave function

$$\Psi = \chi_i \phi_d \phi_A + \chi_f \phi_B^c, \quad (2)$$

where ϕ_d is the deuteron eigenfunction, ϕ_A is the ground state of the target nucleus, and ϕ_B^c represents the c th eigenstate of the final compound nucleus B . These wave functions satisfy

$$\begin{aligned} h_d \phi_d &= (K_{np} + V_{np}) \phi_d = \varepsilon_d \phi_d, \\ h_A \phi_A &= \varepsilon_A \phi_A, \\ h_B \phi_B^c &= (K_n + h_A + V_{An}) \phi_B^c = \varepsilon_B^c \phi_B^c. \end{aligned} \quad (3)$$

Here, K_{np} is the kinetic energy of the neutron-proton motion, and h_A is the internal Hamiltonian of the target nucleus A . In Fig. 1 we define the coordinates that we use in our formulation. These will become useful throughout this section.

Considering only first order in the couplings between the incoming-deuteron channel i and the final-proton channel f , the coupled equations for the unknowns χ_i and χ_f simplify to the distorted-wave Born approximation (DWBA) differential equations and can be written in either prior or post

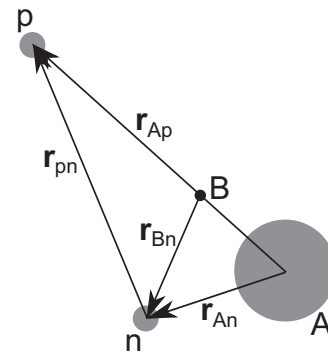


FIG. 1. Definition of coordinates used in our formulations.

form [17],

$$\begin{aligned} (E_i - H_i)\chi_i &= 0, \\ (E_f - H_f)\chi_f &= \left\{ \begin{aligned} &\langle \phi_B^c | V_{\text{prior}} | \phi_d \phi_A \rangle \chi_i \\ &\langle \phi_B^c | V_{\text{post}} | \phi_d \phi_A \rangle \chi_i + (H_f - E_f) \langle \phi_B^c | \phi_d \phi_A \rangle \chi_i, \end{aligned} \right. \end{aligned} \quad (4)$$

where the initial and final Hamiltonians are

$$\begin{aligned} H_i &= K_d + U_{Ad}, \\ H_f &= K_p + U_{Ap}, \end{aligned} \quad (5)$$

with the prior and post operators

$$\begin{aligned} V_{\text{prior}} &= V_{An} + U_{Ap} - U_{Ad}, \\ V_{\text{post}} &= V_{np}, \end{aligned} \quad (6)$$

and the energies $E_i = E - \varepsilon_d - \varepsilon_A$ and $E_f = E - \varepsilon_B^c$. For a target A with a big but finite mass, the *post* form will include a negligible remnant term $U_{Ap} - U_{Bp}$, with U_{Bp} being the optical potential between the proton and the nucleus B . In the approximation in which the proton is treated as a spectator, it is important to note that, in any case, this term does not depend upon the intrinsic coordinates of the target A .

$$\begin{aligned} \frac{d^2\sigma}{d\Omega_p dE_p} &= \frac{2\pi}{\hbar v_d} \rho_p(E_p) \sum_c |\langle \chi_f^{(-)} \phi_B^c | V | \phi_d \phi_A \chi_i \rangle|^2 \delta(E - E_p - \varepsilon_B^c) \\ &= -\frac{2}{\hbar v_d} \rho_p(E_p) \text{Im} \langle \phi_d \phi_A \chi_i | V^\dagger | \chi_f^{(-)} \rangle G_B(\chi_f^{(-)} | V | \phi_d \phi_A \chi_i), \end{aligned} \quad (11)$$

where the round brackets indicate that we only integrate over the proton coordinate. Here, V stands for either V_{prior} or V_{post} ,

$$\rho_p(E_p) = \frac{m_p k_p}{8\pi^3 \hbar^2} \quad (12)$$

is the proton level density, and E_p is the kinetic energy of the detected proton.

The energy-conserving delta function $\delta(E - E_p - \varepsilon_B^c)$ can be written as the imaginary part of the spectral expansion

$$G_B = \lim_{\epsilon \rightarrow 0} \sum_c \frac{|\phi_B^c \rangle \langle \phi_B^c|}{E - E_p - \varepsilon_B^c + i\epsilon}. \quad (13)$$

This Green's function, in operator form, is simply

$$G_B = \frac{1}{E - E_p - h_B + i\epsilon}. \quad (14)$$

Since V_{np} is not contained in h_B , Eq. (14) can be interpreted as a propagator in the breakup channel, i.e., when the deuteron bound state is absent. Furthermore, if we choose the *post* representation of Eq. (11), we have the advantage that the potential $V = V_{\text{post}} = V_{pn}(r_{pn})$ does not depend on ξ_A , so we can directly project the Green's function onto the target ground

state, the so-called optical reduction,

$$X_f = \chi_f + \langle \phi_B^c | \phi_d \phi_A \rangle \chi_i, \quad (7)$$

is such that, in the post representation,

$$(H_f - E_f)X_f = \langle \phi_B^c | V_{\text{post}} | \phi_d \phi_A \rangle \chi_i. \quad (8)$$

The nonorthogonality term $\langle \phi_B^c | \phi_d \phi_A \rangle$ vanishes for large values of the proton coordinate, so X_f and χ_f are asymptotically identical. Therefore, the T matrix T_{dc} for the detection of the proton after the population of the state ϕ_B^c of the residual nucleus has two equivalent expressions:

$$T_{dc} = \langle \chi_f^{(-)} \phi_B^c | V_{\text{prior}} | \phi_d \phi_A \chi_i \rangle = \langle \chi_f^{(-)} \phi_B^c | V_{\text{post}} | \phi_d \phi_A \chi_i \rangle, \quad (9)$$

and the celebrated *post-prior* equivalence in DWBA is verified. The proton distorted wave $\chi_f^{(-)}$ satisfies the equation

$$(E_f - H_f^\dagger)\chi_f^{(-)} = 0. \quad (10)$$

The inclusive cross section is summed over all B channels of a given energy. The inclusive breakup cross section for the process $d + A \rightarrow p + B$ is thus

state, the so-called optical reduction,

$$G_B^{\text{opt}} = \langle \phi_A | G_B | \phi_A \rangle = \frac{1}{E - E_p - \varepsilon_A - K_n - U_{An}(r_{An}) + i\epsilon}. \quad (15)$$

The exact form of U_{An} obtained from the above projection operation is the Feshbach optical potential for the $n - A$ system in the ground state of A and includes the effects of all possible excitations of A due to the interaction with the neutron. In the present paper we use, instead, a global optical potential obtained from a systematic fitting to elastic-scattering data [18]. For both positive and negative energies, this optical potential $U_{An} = V_{An} + iW_{An}$ (with V_{An}, W_{An} real) should be interpreted as an energy-averaged approximation to the exact Feshbach potential.

The inclusive cross section has thus the post-form expression

$$\begin{aligned} \frac{d^2\sigma}{d\Omega_p dE_p} &= -\frac{2}{\hbar v_d} \rho_p(E_p) \text{Im} \langle \phi_d \chi_i | V_{pn} | \chi_f^{(-)} \rangle \\ &\quad \times G_B^{\text{opt}}(\chi_f^{(-)} | V_{pn} | \phi_d \chi_i). \end{aligned} \quad (16)$$

Because the real potential $V_{np}(r_{np})$ cannot excite the nucleus A , this formalism suggests a two-step mechanism: $V_{np}(r_{np})$ first breaks up the deuteron and then G_B^{opt} propagates the system in

the breakup channel, eventually leading to the absorption of the neutron in the complex field U_{An} .

It is useful to extract from Eq. (16) the contributions of breakup without the excitation of the target A (elastic breakup, EB), and nonelastic breakup (NEB) where the target no longer remains in its ground state. To this purpose, we transform

$$\begin{aligned} G_B^{\text{opt}} &= G_0(1 + G_B^{\text{opt}}U_{An}) \\ &= (1 + G_B^{\text{opt}\dagger}U_{An}^\dagger)G_0(1 + G_B^{\text{opt}}U_{An}) - G_B^{\text{opt}\dagger}U_{An}^\dagger G_B^{\text{opt}}, \\ G_B^{\text{opt}\dagger} &= (1 + G_B^{\text{opt}\dagger}U_{An}^\dagger)G_0^\dagger(1 + G_B^{\text{opt}}U_{An}) - G_B^{\text{opt}\dagger}U_{An}^\dagger G_B^{\text{opt}}, \end{aligned} \quad (17)$$

where G_0 is the propagator in free space. We now define the scattering waves $|\chi_n(r_n; k_n)\rangle$ subject to the optical potential U_{An} :

$$|\chi_n(r_{An}; k_n)\rangle = (1 + G_B^{\text{opt}}U_{An})|\chi_0(r_{An}; k_n)\rangle, \quad (18)$$

where $|\chi_0(r_{An}; k_n)\rangle$ is a free plane wave with momentum k_n . From these expressions, we obtain

$$\begin{aligned} \text{Im } G_B^{\text{opt}} &= (1 + G_B^{\text{opt}\dagger}U_{An}^\dagger)\text{Im } G_0(1 + G_B^{\text{opt}}U_{An}) \\ &\quad + G_B^{\text{opt}\dagger}W_{An}G_B^{\text{opt}} \\ &= -\pi \sum_{k_n} |\chi_n(r_n; k_{An})\rangle \delta\left(E - E_p - \frac{k_n^2}{2m_n}\right) \\ &\quad \times \langle \chi_n(r_{An}; k_n) | + G_B^{\text{opt}\dagger}W_{An}G_B^{\text{opt}}. \end{aligned} \quad (19)$$

The first term of Eq. (17), when used in Eq. (16), gives rise to DWBA elastic breakup. For this we have transition matrix elements

$$T_{EB}(\mathbf{k}_n, \mathbf{k}_p) = \langle \chi_f^{(-)} | \chi_n | V_{pn} | \phi_d \chi_i \rangle. \quad (20)$$

The elastic-breakup differential cross section for the protons is given by integrating over the neutron angles:

$$\left. \frac{d^2\sigma}{dE_p d\Omega_p} \right]^{EB} = \frac{2\pi}{\hbar v_d} \rho_p(E_p) \rho_n(E_n) \int |T_{EB}(\mathbf{k}_n, \mathbf{k}_p)|^2 d\Omega_{Bn}, \quad (21)$$

where, in conjunction with the proton density introduced in Eq. (12), we use the neutron density of states

$$\rho_n(E_n) = \frac{m_n k_n}{8\pi^3 \hbar^2}. \quad (22)$$

The second term of Eq. (19) gives rise to the nonelastic-breakup cross section. Defining the post form of the source

term,

$$S_{\text{post}} = \langle \chi_f^{(-)} | V_{pn} | \phi_d \chi_i \rangle, \quad (23)$$

and the neutron wave function

$$|\psi_n^{\text{post}}\rangle = G_B^{\text{opt}} S_{\text{post}}, \quad (24)$$

the nonelastic-breakup differential cross section can then be written as

$$\left. \frac{d^2\sigma}{d\Omega_p dE_p} \right]^{NEB} = -\frac{2}{\hbar v_d} \rho_p(E_p) \langle \psi_n^{\text{post}} | W_{An} | \psi_n^{\text{post}} \rangle. \quad (25)$$

Equation (19) suggests that the elastic and nonelastic breakup have a common origin. In Appendix A, we show that flux-conservation laws give rise to separate elastic and nonelastic terms in a consistent manner.

B. General formalism in the *prior* representation (UT)

Computing the neutron wave function (24) presents well-known numerical difficulties. Because the deuteron wave function ϕ_d and the *post* potential V_{pn} have the same argument, the source term (23) oscillates indefinitely as a function of the neutron coordinate, and the integral in Eq. (25) converges exceedingly slowly. There are methods to deal with this numerical problem. Alternatively we follow Udagawa and Tamura (UT) and revert to the *prior* representation. Let us first write the inclusive cross section in the prior representation:

$$\begin{aligned} \left. \frac{d^2\sigma}{d\Omega_p dE_p} \right] &= -\frac{2}{\hbar v_d} \rho_p(E_p) \text{Im} \langle \phi_d \phi_A \chi_i | V_{\text{prior}}^\dagger | \chi_f^{(-)} \rangle \\ &\quad \times G_B(\chi_f^{(-)} | V_{\text{prior}} | \phi_d \phi_A \chi_i), \end{aligned} \quad (26)$$

where $V_{\text{prior}} = V_{An} + U_{Ap} - U_d$ is the prior interaction potential [see Eq. (6)]. Now, however, the optical reduction defined by Eq. (15) cannot be readily applied, because V_{prior} acts on the intrinsic coordinates ξ_A of the nucleus A and does not commute with ϕ_A .

We will thus split V_{prior} into a term that can induce breakup (and commutes with ϕ_A) and a term that can excite ϕ_A (and commutes with $\chi_f^{(-)}$):

$$\begin{aligned} V_{\text{prior}} &= (G_B^{-1} + V_{\text{prior}}) - G_B^{-1} \\ &= (U_{Ap} - U_{Ad} - h_A - K_n - E_p + E) - G_B^{-1}. \end{aligned} \quad (27)$$

Note that, when doing the averaging over the states of the target, some terms drop out. Introducing $\Delta U = U_{Ap} - U_{Ad}$, we can write

$$\begin{aligned} \langle \phi_A | V_{\text{prior}}^\dagger | \chi_f \rangle G_B(\chi_f^{(-)} | V_{\text{prior}} | \phi_A) &= (\Delta U^\dagger - K_n + E_n) |\chi_f^{(-)}\rangle G_B^{\text{opt}}(\chi_f^{(-)} | (\Delta U - K_n + E_n) \\ &\quad + |\chi_f^{(-)}\rangle (K_n - \bar{V}_{An} - E_n) \langle \chi_f^{(-)} | + (\Delta U^\dagger + \Delta U) |\chi_f^{(-)}\rangle \langle \chi_f^{(-)} |, \end{aligned} \quad (28)$$

where $E_n = E - E_p - \varepsilon_A$ and $\bar{V}_{An} = \langle \phi_A | V_{An} | \phi_A \rangle$. When taking the imaginary part in Eq. (26), the last term in Eq. (28) gives no contribution since it is a real operator. If we substitute $E_n - K_n$ with U_{An} , we have

$$\text{Im} \langle \phi_A | V_{\text{prior}}^\dagger | \chi_f \rangle G_B(\chi_f^{(-)} | V_{\text{prior}} | \phi_A) = (\Delta U^\dagger + U_{An}) |\chi_f^{(-)}\rangle G_B^{\text{opt}}(\chi_f^{(-)} | (\Delta U + U_{An}) + |\chi_f^{(-)}\rangle (U_{An} - \bar{V}_{An}) \langle \chi_f^{(-)} |. \quad (29)$$

It is convenient to rewrite Eq. (29) in the following form:

$$\begin{aligned} \text{Im}\langle\phi_A|V_{\text{prior}}^\dagger|\chi_f^{(-)}\rangle G_B(\chi_f^{(-)}|V_{\text{prior}}|\phi_A) &= (\Delta U + U_{An})^\dagger|\chi_f^{(-)}\rangle G_B^{\text{opt}}(\chi_f^{(-)}|(\Delta U + U_{An}) \\ &+ 2iW_{An}|\chi_f^{(-)}\rangle G_B^{\text{opt}}(\chi_f^{(-)}|(\Delta U + U_{An}) + |\chi_f^{(-)}\rangle(U_{An} - \bar{V}_{An})(\chi_f^{(-)}|. \end{aligned} \quad (30)$$

The substitution of $E_n - K_n$ with U_{An} might seem dubious because, even if it is clear from the first line of Eq. (11) that we are dealing with on-shell quantities, the second line seems to formally include off-shell terms. But, if we consider $E_n - K_n = (G_B^{\text{opt}})^{-1} + U_{An}$, we can see that the off-shell term $(G_B^{\text{opt}})^{-1}$ gives a real contribution to Eq. (28) and vanishes when taking the imaginary part in Eq. (26).

It is now convenient to define the prior-form source term

$$S_{\text{prior}} = (\chi_f^{(-)}|\Delta U + U_{An}|\phi_d\chi_i). \quad (31)$$

Note that the operator $\Delta U + U_{An}$ differs from the prior interaction defined in Eq. (6); namely, the complex optical potential U_{An} is used instead of the real interaction V_{An} that causes core excitation. The prior-form neutron wave function is

$$\psi_n^{\text{prior}} = G_B^{\text{opt}} S_{\text{prior}}. \quad (32)$$

We also need to introduce the nonorthogonality function:

$$\psi_n^{\text{HM}} = (\chi_f^{(-)}|\phi_d\chi_i). \quad (33)$$

This last expression defines the neutron ‘‘source’’ function obtained by Hussein and McVoy (HM) using somewhat different approximations [10]. Now, inserting Eq. (30) into Eq. (26), we arrive at

$$\begin{aligned} \frac{d^2\sigma}{d\Omega_p dE_p} &= -\frac{2}{\hbar v_d} \varphi(E_p) [\text{Im}\langle S_{\text{prior}}|G_B^{\text{opt}}|S_{\text{prior}}\rangle \\ &+ 2\text{Re}\langle\psi_n^{\text{HM}}|W_{An}G_B^{\text{opt}}|S_{\text{prior}}\rangle \\ &+ \langle\psi_n^{\text{HM}}|W_{An}|\psi_n^{\text{HM}}\rangle]. \end{aligned} \quad (34)$$

We can apply the identity (19) to remove from the first term of Eq. (34) the elastic-breakup contribution. The remaining terms represent the total nonelastic-breakup cross section:

$$\begin{aligned} \left. \frac{d^2\sigma}{d\Omega_p dE_p} \right]_{\text{NEB}} &= -\frac{2}{\hbar v_d} \rho_p(E_p) [\text{Im}\langle\psi_n^{\text{prior}}|W_{An}|\psi_n^{\text{prior}}\rangle \\ &+ 2\text{Re}\langle\psi_n^{\text{HM}}|W_{An}|\psi_n^{\text{prior}}\rangle \\ &+ \langle\psi_n^{\text{HM}}|W_{An}|\psi_n^{\text{HM}}\rangle]. \end{aligned} \quad (35)$$

The first term corresponds to elastic breakup followed by capture, while the third term contains all other processes involving the $n + A$ system. As we will show, all three terms are, in general, important and have to be simultaneously taken into account. For completeness, we present in Appendix B the partial wave decomposition of these results.

We have just shown that the nonorthogonality term in the above expression arises when disentangling the elastic- and nonelastic-breakup contributions from V_{prior} . On the other hand, an identical nonorthogonality function appears for different reasons in the derivation of the standard DWBA

equations in the post form but has been dropped because of the equivalence of the final (proton channel) distorted waves X_f and χ_f in the asymptotic region [see Eq. (7)]. Nonetheless, in Eq. (25) the proton distorted wave is certainly needed for small values of the proton coordinate, so the question may arise whether the latter nonorthogonality function should be kept after all for its derivation.

To see that such a term is actually not needed, let us check the consequences of including it. By examining Eq. (4), it can be seen that this is equivalent to making the replacement

$$V \rightarrow V_{pn} + (K_p + U_{Ap} + h_B - E) \quad (36)$$

in Eq. (11). We obtain the following from the post-form matrix element in Eq. (11):

$$\begin{aligned} \langle\phi_d\phi_A\chi_i|V_{pn} + (K_p + U_{Ap}^\dagger + h_B - E)|\chi_f^{(-)}\rangle G_B \\ \times (\chi_f^{(-)}|(V_{pn} + (K_p + U_{Ap} + h_B - E)|\phi_d\phi_A\chi_i) \\ = \langle\phi_A|[S_{\text{post}}^* + \psi_n^{\text{HM}*}(h_B + E_p - E)] \\ \times G_B[S_{\text{post}} + \psi_n^{\text{HM}}(h_B + E_p - E)]|\phi_A\rangle, \end{aligned}$$

where we have used Eqs. (10) and (24). Taking into account that $(h_B + E_p - E)G_B = \mathbb{1}$, we get

$$\begin{aligned} S_{\text{post}}^* G_B^{\text{opt}} S_{\text{post}} + 2\text{Re}(S_{\text{post}}\psi_n^{\text{HM}}) \\ + \langle\phi_A|S_{\text{post}}^*(h_B + E_p - E)S_{\text{post}}|\phi_A\rangle. \end{aligned} \quad (37)$$

When taking the imaginary part, only the first term of the above expression survives, and we obtain again Eq. (16). We conclude that the post-source term defined in Eq. (23) should not include a nonorthogonality contribution.

C. Transfer to bound states

The sort of breakup processes we are considering can be thought of as transfer to the continuum. One would like to have one framework to describe both transfer to bound states and continuum states. The Green’s function formalism allows for this connection. This idea was first proposed in Ref. [15]. We write the partial wave coefficients of the Green’s function $G_B^{\text{opt}}(\mathbf{r}_{An}, \mathbf{r}'_{An})$ defined in Eq. (15) as

$$G_l(r_{An}, r'_{An}) = \frac{f_l(k_n, r_{An<})g_l(k_n, r_{An>})}{k_n r_{An} r'_{An}}, \quad (38)$$

where $k_n = \sqrt{2m_n \varepsilon}/\hbar$, and $f_l(k_n, r_{An})[g_l(k_n, r_{An})]$ is the regular (irregular) solution of the homogeneous equation

$$\begin{aligned} \left(-\frac{\hbar^2}{2m_n} \frac{d^2}{dr_{An}^2} + U_{An}(r_{An}) + \frac{\hbar^2 l(l+1)}{2m_n r_{An}^2} - \varepsilon \right) \\ \times \{f_l, g_l\}(k_n, r_{An}) = 0. \end{aligned} \quad (39)$$

At the origin we impose $\lim_{r_{An} \rightarrow 0} f_l(k_n, r_{An}) = 0$ for the regular solution. At large distances the boundary condition of course

depends on whether the energy ε is positive or negative. For scattering neutron states (positive ε),

$$\lim_{r_{An} \rightarrow \infty} g_l(k_n, r_{An}) \rightarrow e^{i(k_n r_{An} - \frac{l\pi}{2})}, \quad (40)$$

while for final neutron bound states (negative ε),

$$\lim_{r_{An} \rightarrow \infty} g_l(k_n, r_n) \rightarrow e^{-\kappa_n r_{An}}, \quad (41)$$

with $\kappa_n = \sqrt{-2m_n \varepsilon}/\hbar$.

If the imaginary part W_{An} of the neutron-target optical potential is small, we can use first-order perturbation theory to express

$$G_B^{\text{opt}}(\mathbf{r}_{An}, \mathbf{r}'_{An}; E) \approx \frac{\hbar^2}{2m_n} \sum_n \frac{\phi_n^*(\mathbf{r}'_{An}) \phi_n(\mathbf{r}_{An})}{E_n + i\Gamma_n/2 - E}, \quad (42)$$

where

$$\Gamma_n = 2 \int \phi_n^* W_{An} \phi_n d\mathbf{r}_{An}, \quad (43)$$

and ϕ_n , E_n are the eigenfunctions and eigenvalues of the Schrödinger equation corresponding to the *real* part of the optical potential. If we now consider an energy E close to an isolated resonance, i.e., $|E - E_n| \ll |E_m - E_n|$, only the n th term of the sum will contribute to the Green's function, and

$$G_B^{\text{opt}}(\mathbf{r}_{An}, \mathbf{r}'_{An}; k) \approx \frac{\hbar^2}{2m_n} \frac{\phi_n^*(\mathbf{r}'_{An}) \phi_n(\mathbf{r}_{An})}{E_n + i\Gamma_n/2 - E}. \quad (44)$$

The resulting neutron wave function is

$$\psi(\mathbf{r}_{An}) = \frac{\hbar^2}{2m_n} \frac{\phi_n(\mathbf{r}_{An})}{E_n + i\Gamma_n/2 - E} \int \phi_n^*(\mathbf{r}'_{An}) S(\mathbf{r}'_{An}) d\mathbf{r}'_{An}. \quad (45)$$

According to the particular nature of the source term [see Eqs. (23) and (31)], the integral in Eq. (45) has the form of a one-neutron-transfer DWBA amplitude,

$$T_n^{(\text{INT})} = \int \phi_n^* S_n d\mathbf{r}'_{An} = \int \phi_n^* (\chi_f^{(-)} | V_{\text{post,prior}} | \phi_d \chi_i) d\mathbf{r}'_{An}, \quad (46)$$

to the single-particle state ϕ_n of the target-neutron residual nucleus. We can then write

$$\psi_n(\mathbf{r}_{An}) = \frac{T_n^{(\text{INT})}}{E_n + i\Gamma_n/2 - E} \phi_n(\mathbf{r}_{An}), \quad (47)$$

and the final neutron wave function $\psi_n(\mathbf{r}_{An})$ can be interpreted as the n th eigenstate of the neutron-target (real) single-particle potential times the direct transfer amplitude to this particular state, modulated by an energy denominator. The absorption cross section is proportional to the matrix element

$$\begin{aligned} \langle \psi | W_{An} | \psi \rangle &= \frac{|T_n^{(\text{INT})}|^2}{(E_n - E)^2 + \Gamma_n^2/4} \int \phi_n^* W_{An} \phi_n d\mathbf{r}_{An} \\ &= \frac{1}{2} \frac{\Gamma_n}{(E_n - E)^2 + \Gamma_n^2/4} |T_n^{(\text{INT})}|^2. \end{aligned} \quad (48)$$

As a consequence, if the transfer amplitude $T_n^{(\text{INT})}$ is approximately constant in an energy interval of the order of Γ_n , the

energy-dependent differential cross section around a resonance has a Lorentzian shape, and the integrated cross section under the peak is independent of W_{An} for small enough W_{An} .

It can be shown (see Appendix C) that there is a simple relationship between the cross section for the capture of a neutron in a bound state of finite width and the cross section for direct transfer to the corresponding zero-width bound state. Assuming again that $T_n^{(\text{INT})}$ is essentially constant in an energy range of the order of $\Gamma_n = 2\langle W_{An} \rangle$, we have

$$\left. \frac{d^2\sigma}{d\Omega_p dE_p} (E, \Omega) \right]^{(\text{NEB})} \approx \frac{1}{2\pi} \frac{\Gamma_n}{(E_n - E)^2 + \Gamma_n^2/4} \frac{d\sigma_n}{d\Omega}(\Omega), \quad (49)$$

where $\frac{d\sigma_n}{d\Omega}$ is the direct-transfer differential cross section to the n th eigenstate of the real potential. At the resonance energy peak ($E = E_n$), we have the simple relationship

$$\left. \frac{d^2\sigma}{d\Omega_p dE_p} (E = E_n, \Omega) \right]^{(\text{NEB})} \approx \frac{2}{\Gamma_n \pi} \frac{d\sigma_n}{d\Omega}(\Omega). \quad (50)$$

III. RESULTS

A. Numerical details

We present the results obtained for the reaction $^{93}\text{Nb}(d, p)$ at two different beam energies, $E_d = 15$ MeV and $E_d = 25.5$ MeV. The optical-model potentials U_{Ad} , U_{Ap} used in the initial (deuteron) and final (proton) channels, respectively, were taken from the Perey and Perey compilation [19] and are summarized in Table I. For the final-state interaction U_{An} between the neutron and the ^{93}Nb target, we have slightly modified the energy-dependent Koning–Delaroche global optical nucleon-nucleus potential [18] by setting the real-part parameter to $V = 50.3$ MeV over the whole energy range and keeping the original energy dependence of the other parameters. This was needed to reproduce essential features of the ^{94}Nb nucleus. Furthermore, although we respect the energy dependence of the depth of the surface imaginary part W_D of the Koning–Delaroche potential, we do not let it fall below 4 MeV, corresponding to the experimental energy resolution of the data in Ref. [16]. The maximum partial wave l_p used in the calculations is 15 and 20 for $E_d = 15$ MeV and $E_d = 25.5$ MeV, respectively. The contribution of final neutron states with $l \geq 8$ is found to be very small.

The deuteron ground-state wave function is taken to be an $L = 0$ state with a radial wave function generated by a Woods–Saxon potential with radius $R_d = 0.4$ fm and diffusivity $a_d = 0.6$ fm. When the real depth is adjusted to

TABLE I. Optical-model parameters. Energies are expressed in MeV and lengths in fm. In the proton channel, the parameters are those listed in Ref. [19] for proton- ^{93}Nb scattering at 16.2 MeV, while in the deuteron channel they correspond to those listed in the same reference for deuteron- ^{93}Nb scattering at 17 MeV.

| | V | W | W_D | a | a_D | r | r_D | r_C |
|-----|------|-----|-------|-------|-------|------|-------|-------|
| d | 99.0 | 0.0 | 16.7 | 0.84 | 0.64 | 1.12 | 1.31 | 1.30 |
| p | 50.6 | 0.0 | 14.1 | 0.678 | 0.47 | 1.25 | 1.25 | 1.25 |

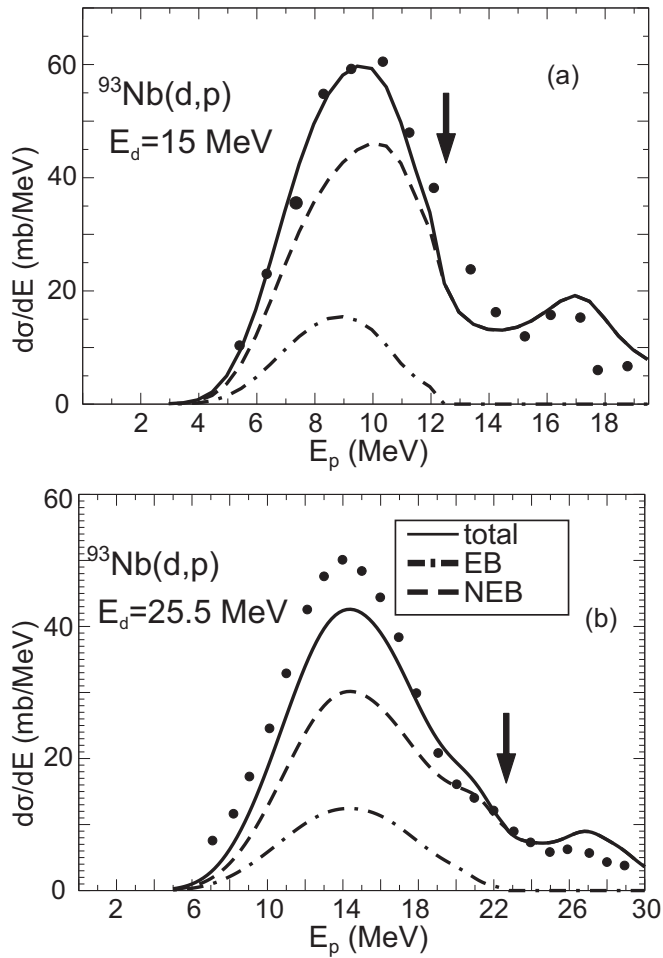


FIG. 2. Energy distributions of the detected proton for $^{93}\text{Nb}(d,p)$ at (a) 15 MeV and (b) 25.5 MeV: total cross sections (solid line), elastic breakup (EB, dot-dashed line), and inelastic breakup (NEB, dashed line). The arrows indicate the position of the neutron emission threshold. Data are from Ref. [16].

reproduce the binding energy of a deuteron, the resulting wave function is compatible with the experimental value of the mean-square radius of the deuteron and the zero-range constant $D_0 = -122.5 \text{ MeV fm}^{3/2}$.

In Fig. 2 we show the proton energy distributions for $^{93}\text{Nb}(d,p)$ at 15 MeV and 25.5 MeV along with the data [16]. Also shown is the breakdown into elastic breakup (EB) and inelastic breakup (NEB). Our results indicate that the inelastic breakup is dominant at all energies, nevertheless elastic breakup is important particularly around the peak of the distribution. The comparison with the data demonstrates that our model provides a good account of the process. A close comparison with the theoretical results presented in Ref. [16] show significant differences that can be partially attributed to the neglect of the additional terms arising from nonorthogonality.

We also compared our results with those from Ref. [13]. At the peak of our distribution for the higher beam energy ($E_p = 14 \text{ MeV}$), the elastic breakup contributes 25% of the total cross section. This differs significantly from the results presented in

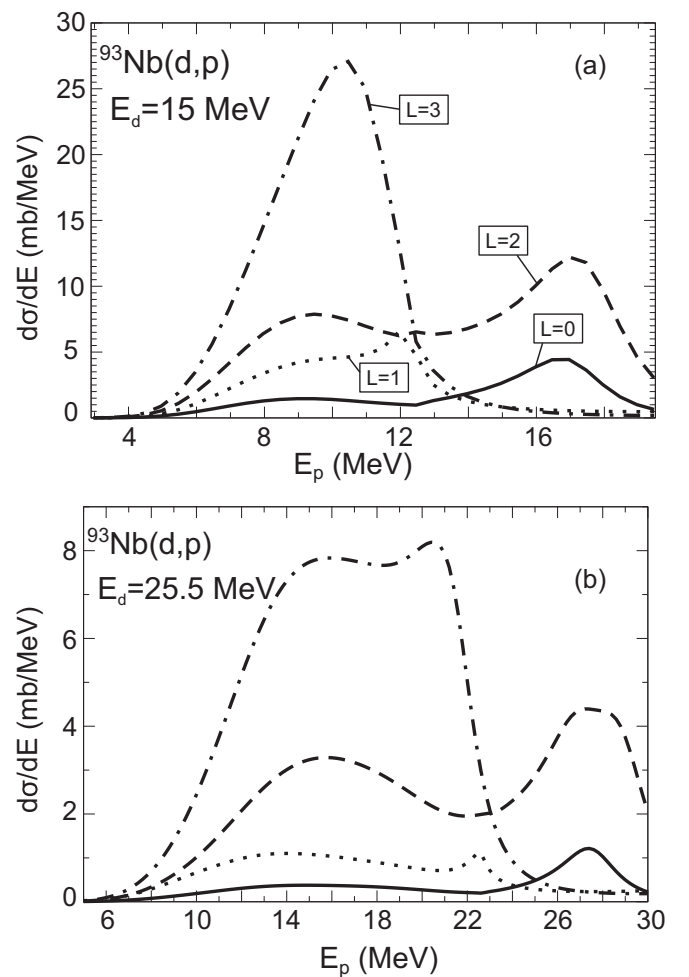


FIG. 3. Energy distributions for $^{93}\text{Nb}(d,p)$ at (a) 15 MeV and (b) 25.5 MeV: partial wave decomposition.

Ref. [13], where the elastic breakup is less than 10% of the total cross section at the peak. This is an important issue because elastic breakup will not lead to the neutron being captured into a compound state and therefore will need to be subtracted from the total cross section in order to apply the surrogate method. In the work of Ref. [13], the elastic breakup is treated in a separate formalism; namely, with the continuum-discretized coupled-channel method. In addition, given that the inelastic contribution is computed in the post formalism, the authors used continuum bins to address the convergence issues. A more detailed comparison between these two methods will be very useful.

For the surrogate method, the spin distributions of the (d,p) cross sections are important in making the connection to neutron capture (see Sec. I). In Fig. 3 we provide the breakdown in terms of the various angular momenta for both beam energies considered. A strong peak is found around $E_p = 10 \text{ MeV}$ for $L = 3$, corresponding to a narrow resonance in the neutron-target system. A much broader resonance is present in the $L = 1$ channel and therefore the peak in that component is less pronounced. For $L = 0$ and $L = 2$, we can see the signature of the neutron-target bound states, at high

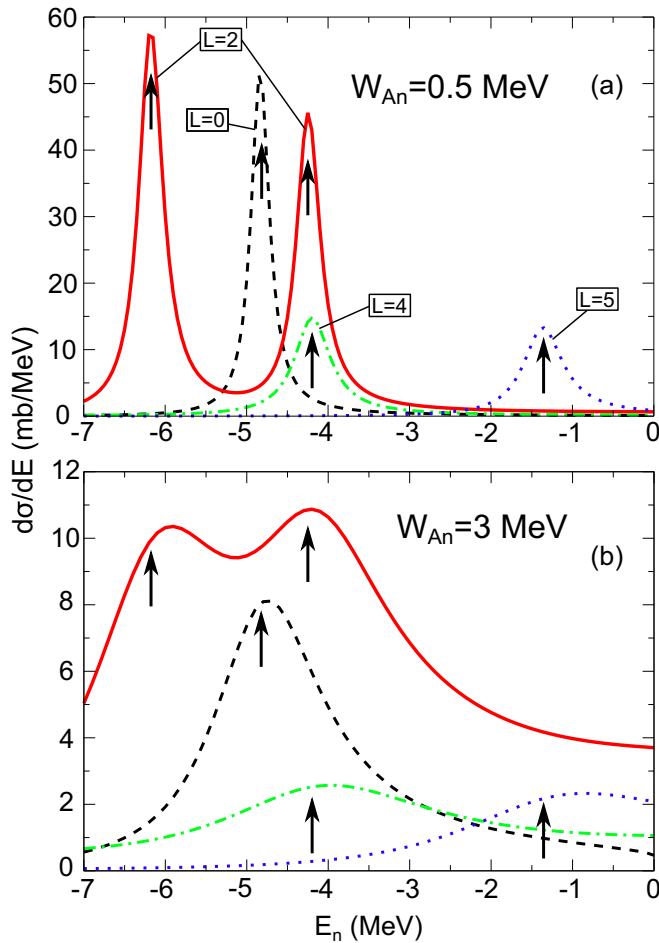


FIG. 4. (Color online) Energy distributions for $^{93}\text{Nb}(d,p)$ at 15 MeV below the neutron threshold for those partial waves that have bound states: (a) strength of the imaginary potential $W = 0.5$ MeV, and (b) strength of the imaginary potential $W = 3.0$ MeV.

proton energy. From the distributions in Fig. 3, it is obvious that the Weisskopf approximation, typically used in the analysis of surrogate reactions, is not valid. The cross section is strongly dependent on the angular momentum and closely connected to the internal structure of the composite final state.

One attractive feature of the model developed here is the ability to provide, in a consistent framework, a description of neutron capture into the continuum and into bound states. The optical potential used to describe the n -target system is primarily based on fits to elastic scattering, appropriate for positive energies, but our results depend on the continuation of the potential to negative energies. In Figs. 2 and 3, for the highest proton energies, corresponding to the neutron below threshold, we keep $W_D = 4$ MeV, as stated above, to describe limited experimental resolution. In Fig. 4, by contrast, we explore the effects of smaller imaginary terms in U_{An} in the $^{93}\text{Nb}(d,p)$ reaction, by changing this value to $W_D = 0.5$ MeV [Fig. 4(a)] and $W_D = 3$ MeV [Fig. 4(b)]. For the smallest imaginary term, bound states appear as narrow peaks. Increasing the imaginary term increases their widths. An example of this can be seen for the $L = 2$ states:

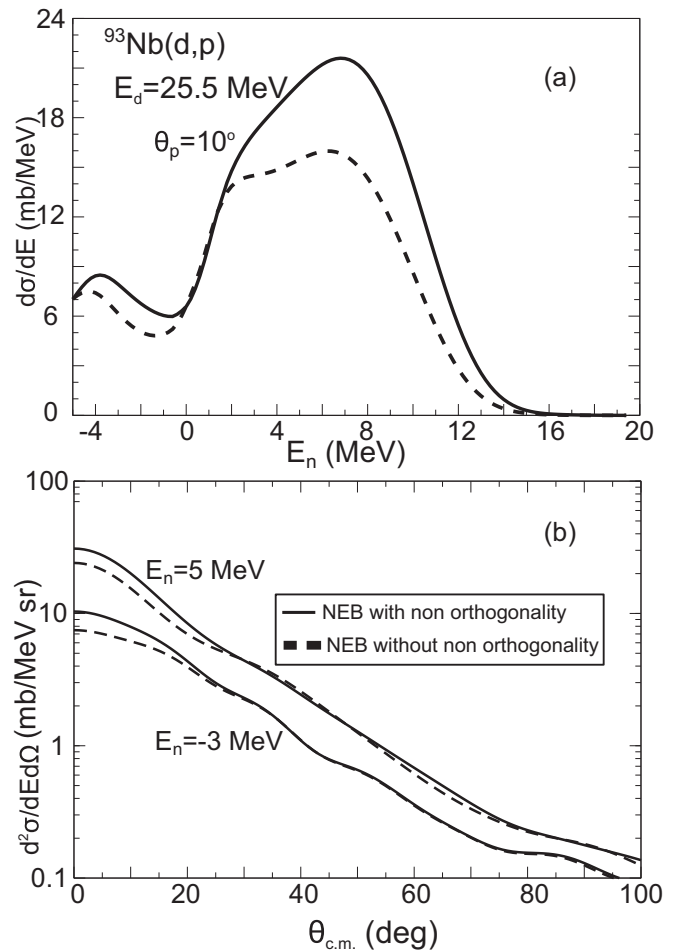


FIG. 5. Effect of the nonorthogonality and cross terms in the cross sections: (a) energy distribution for $^{93}\text{Nb}(d,p)$ at 25.5 MeV for an angle $\theta = 10^\circ$ and (b) angular distributions for both $E_n = -3$ MeV and $E_n = 5$ MeV.

when the imaginary term is small, we can resolve the $L = 2$ spin-orbit partners, while as we increase the imaginary term, these two states become blurred to the point of becoming indistinguishable in Fig. 3. The arrows in Fig. 3 correspond to the location of the bound states for the real potential. We find that that, in addition to the spreading of the states, the introduction of the imaginary component can also shift the peaks to higher energy. As discussed in Sec. II C, the limit of $W_D = 0$ MeV in our formulation corresponds to the standard DWBA transfer to bound states. We have indeed used this fact to check our calculations by comparing our results in this limit to those produced by FRESKO [20]. Complete agreement was found.

The basis of the large controversy between the AV and the UT approaches stems from the nonorthogonality term, discussed in detail in Sec. II B. It is therefore critical to understand the importance of this term in the calculations. In Fig. 5 we plot the inelastic-breakup cross sections with (solid line) and without (dashed line) the nonorthogonality term. The neutron energy distribution, for $\theta_p = 10^\circ$, is shown in [Fig. 5(a)] and the angular distribution, for two neutron energies, is shown in

[Fig. 5(b)]. The nonorthogonality term is most important at the peak of the energy distribution but remains important even when the neutron is captured into bound states. In terms of the angular distribution, the nonorthogonality term manifests itself mostly at forward angles. The results in Fig. 5 demonstrate the need for the inclusion of the nonorthogonality term in the prior-form formalism. The discrepancies found in the literature between the AV and the UT approaches are, to a large extent, a consequence of the fact that UT neglects the nonorthogonality term.

IV. CONCLUSIONS

We have derived, implemented, and validated a practical theory for computing cross sections for inclusive processes of the type $A(d, p)X$, where only the proton is detected in the final state. This includes elastic breakup as well as all other inelastic processes. Our model is based on the assumption that the proton is a spectator and cannot excite the target. The same framework is able to describe these reactions across the full neutron-energy range in a consistent manner. Our model is directly relevant to the application of the surrogate method for extracting neutron-capture cross sections from (d, p) reactions. The present formalism can be generalized to describe the partial fusion of any cluster in a loosely bound projectile.

We discuss in detail the post and the prior formalisms. While the cross sections derived in the post form are formally more elegant, they pose convergence challenges. This challenge is removed in the prior formalism. However, additional terms due to nonorthogonality arise. We show that these terms are important and cannot be neglected for all energies of the detected proton. We also predict the spin distribution of the resulting compound nucleus, an important ingredient for the application of the surrogate method to extract neutron-capture reactions. We show that the cross sections are strongly dependent on the angular momentum, a factor that needs to be incorporated in the analysis of the surrogate data. Finally, we also make predictions regarding the relative contribution of the elastic breakup and all other inelastic processes. The elastic-breakup process does not lead to neutron capture and needs to be subtracted from the total (d, p) cross section when relating it back to (n, γ) . In this work, we have resolved a decades-old controversy; namely, that between Austern *et al.* and Udagawa *et al.*, promulgating respectively the post and the prior methods for describing the inclusive process $A(d, p)X$.

While our method is able to describe the one example we study, it is important to perform a systematic study for various nuclei across the nuclear chart. Also, since our method makes consistent predictions for both the elastic and inelastic breakup, it would be very useful to have the measurement of elastic breakup for the same cases that have been studied with the inclusive experiments.

In comparing our methods with other calculations, we found small differences with Ref. [16], which can be partially attributed to the neglect of the nonorthogonality-induced terms. More concerning, we found significant differences with the predictions of Ref. [13], particularly in the elastic-breakup cross section. Given that, in Ref. [13], the elastic breakup was obtained through a different formalism, the comparison is

not straightforward. Nevertheless, a better understanding on the source of the differences is desirable. Again, elastic-breakup data for these cases would be useful.

Obtaining a reliable cross section for processes of the type $A(d, p)X$ is only the first step in the application of the surrogate method. The elastic-breakup cross section needs to be subtracted from the total cross section, and the remaining cross section needs to be treated within a statistical approach to determine the fraction of neutrons that end up being captured versus those that evaporate. The coupling to a statistical method is planned for the near future.

ACKNOWLEDGMENTS

We are grateful to Jutta Escher for useful discussions. This work was supported by the National Science Foundation under Grant No. PHY-1403906, by the Department of Energy, Office of Science, Office of Nuclear Physics under Award No. DE-FG52-08NA28552, and by Lawrence Livermore National Laboratory under Contract DE-AC52-07NA27344.

APPENDIX A: DISCUSSION OF EB AND NEB IN THE CONTEXT OF FLUX CONVERSATION

We rewrite the differential equation for the neutron wave function (24) in the following form:

$$(\nabla^2 + \bar{U}_{An} - \bar{E})\psi_n^{\text{post}} = \bar{S}_{\text{post}}, \quad (\text{A1})$$

where

$$\bar{S}_{\text{post}} = \frac{2m_n}{\hbar^2} S_{\text{post}}, \quad (\text{A2})$$

and $\bar{U}_{An} = \frac{2m_n}{\hbar^2} U_{An}$, $\bar{E} = \frac{2m_n}{\hbar^2} (E - E_p - \varepsilon_A)$. From Eq. (A1) and its complex conjugate, and multiplying respectively by $\psi_n^{\text{post}*}$ and ψ_n^{post} , we get (we drop the ‘‘post’’ suffix)

$$\begin{aligned} \psi_n^* (\nabla^2 + \bar{U}_{An} - \bar{E}) \psi_n &= \psi_n^* \bar{S}, \\ \psi_n (\nabla^2 + \bar{U}_{An}^\dagger - \bar{E}) \psi_n^* &= \psi_n \bar{S}^\dagger. \end{aligned} \quad (\text{A3})$$

Taking the difference between the above equations and integrating over a large volume, we obtain

$$\begin{aligned} \int \nabla \cdot (\psi_n \nabla \psi_n^* - \psi_n^* \nabla \psi_n) d\mathbf{r}_n - 2i \int |\psi_n|^2 \bar{W}_{An} d\mathbf{r}_n \\ = 2i \int \text{Im}(\psi_n \bar{S}^\dagger) d\mathbf{r}_n. \end{aligned} \quad (\text{A4})$$

The first term can be cast into an outgoing elastic flux across the surface enclosing the volume, while the second term accounts for the nonelastic breakup. The above equation describes how the flux generated by the right-hand-side term is converted into an elastic and a nonelastic contribution.

APPENDIX B: PARTIAL WAVE DECOMPOSITION OF DIFFERENTIAL CROSS SECTION

After partial wave decomposition, the multiple differential cross section can thus be written in the prior and post forms,

$$\frac{d^2\sigma}{d\Omega_p dE_p} = \frac{2\pi}{\hbar v_d} \rho_p(E_p) \sum_{l,m} B_{lm}^{\text{prior,post}}, \quad (\text{B1})$$

where the post contributions are

$$B_{lm}^{\text{post}} = \int \left| \sum_{l_p} \phi_{lm_l p}^{\text{post}}(r_{Bn}; k_p) Y_{-m}^{l_p}(\theta_p) \right|^2 W_{An}(r_{An}) dr_{Bn}, \quad (\text{B2})$$

and the prior contributions

$$\begin{aligned} B_{lm}^{\text{prior}} &= \int \left| \sum_{l_p} \phi_{lm_l p}^{\text{prior}}(r_{Bn}; k_p) Y_{-m}^{l_p}(\theta_p) \right|^2 W_{An}(r_{An}) dr_{Bn} \\ &+ \int \left| \sum_{l_p} \phi_{lm_l p}^{\text{HM}}(r_{Bn}; k_p) Y_{-m}^{l_p}(\theta_p) \right|^2 W_{An}(r_{An}) dr_{Bn} \\ &- 2\text{Re} \int \sum_{l_p, l'_p} \phi_{lm_l p}^{\text{HM}}(r_{Bn}; k_p) \phi_{lm'_l p}^{\text{prior}*}(r_{Bn}; k_p) \\ &\times Y_{-m}^{l_p}(\theta_p) Y_{-m}^{l'_p}(\theta_p) W_{An}(r_{An}) dr_{Bn}. \end{aligned} \quad (\text{B3})$$

Here we have used the neutron partial wave functions, equivalently for prior or post,

$$\psi_n(\mathbf{r}_{Bn}; \mathbf{k}_p) = \sum_{l, m, l_p} \phi_{lm_l p}(r_{Bn}; k_p) Y_m^l(\theta_{Bn}) Y_{-m}^{l_p}(\theta_p) / r_{Bn}, \quad (\text{B4})$$

with the source terms having a similar decomposition,

$$S(\mathbf{r}_n; \mathbf{k}_p) = \sum_{lm_l p} s_{lm_l p}(r_n; \mathbf{k}_p) Y_{lm}(\theta_{Bn}) Y_{l_p m}(\theta), \quad (\text{B5})$$

so

$$\begin{aligned} \phi_{lm_l p}(r_{An}, k_p) &= \int G_l(r_{An}, r'_{An}) s_{lm_l p}(r'_{An}; k_p) r_{An}^2 dr'_{An} \\ &= \frac{1}{k_n} \left(g_l(k_n, r_{An}) \int_0^{r_{An}} f_l(k_n, r'_{An}) \right. \\ &\quad \times s_{lm_l p}(r'_{An}; k_p) r'_{An} dr'_{An} + f_l(k_n, r_{An}) \\ &\quad \times \int_{r_{An}}^{\infty} g_l(k_n, r'_{An}) s_{lm_l p}(r'_{An}; k_p) r'_{An} dr'_{An} \Big). \end{aligned} \quad (\text{B6})$$

APPENDIX C: TRANSFER CROSS SECTIONS TO BOUND STATES

In this Appendix we show that the value of the integrated cross section under the peak in Eq. (49) is equal to the direct-transfer cross section to a sharp bound state. Let us consider the limit

$$\lim_{W_{An} \rightarrow 0} \langle \psi | W_{An} | \psi \rangle = \pi |T_n^{(\text{INT})}|^2 \delta(E_n - E), \quad (\text{C1})$$

and substitute Eq. (C1) into Eq. (25),

$$\begin{aligned} \left. \frac{d^2 \sigma}{d\Omega_p dE_p} \right]_{\text{NEB}} &= -\frac{m_d m_p k_p}{4\pi^2 \hbar^4 k_d} \langle \psi_n | W_{An} | \psi_n \rangle \\ &= \frac{m_d m_p k_p}{4\pi^2 \hbar^4 k_d} |T_n^{(\text{INT})}|^2 \delta(E_n - E), \end{aligned} \quad (\text{C2})$$

where the subindices p, d refer to the proton and the deuteron, respectively, and we have used the density of levels (12). If we integrate over a vanishing interval δE around E_n , we get

$$\left. \frac{d\sigma}{d\Omega_p} \right]_{\text{NEB}} = \frac{m_d m_p k_p}{4\pi^2 \hbar^4 k_d} |T_n^{(\text{INT})}|^2, \quad (\text{C3})$$

which is the DWBA transfer differential cross section.

Moreover, in this limit the nonorthogonality term and the cross term vanish. Indeed, the functions $\phi_{lm_l p}^{\text{HM}}(r_{Bn}; k_p)$, not being affected by the propagator, do not exhibit any resonant behavior around the poles E_n . Thus the second term in Eq. (B3) vanishes as $W_{An} \rightarrow 0$. On the other hand, the third term behaves as

$$\sim \lim_{\Gamma_n \rightarrow 0} \frac{\Gamma_n}{(E_n - E) + i\Gamma_n/2} \quad (\text{C4})$$

when $W_{An} \rightarrow 0$ and is equal to zero everywhere except in the zero-measure interval around $E_n = E$, where it has the finite value $-2i$. Its contribution thus vanishes after the energy integration. In addition, the interaction U_{An} used in the prior representation (see Sec. II B) coincides now with the real potential V_{An} , so the standard post-prior symmetry is fully recovered.

-
- [1] J. E. Escher, J. T. Burke, F. S. Dietrich, N. D. Scielzo, I. J. Thompson, and W. Younes, *Rev. Mod. Phys.* **84**, 353 (2012).
[2] R. Hatarik, L. A. Bernstein, J. A. Cizewski, D. L. Bleuel, J. T. Burke, J. E. Escher, J. Gibelin, B. L. Goldblum, A. M. Hatarik, S. R. Leshner *et al.*, *Phys. Rev. C* **81**, 011602 (2010).
[3] A. Kerman and K. McVoy, *Ann. Phys. (NY)* **122**, 197 (1979).
[4] T. Udagawa and T. Tamura, *Phys. Rev. Lett.* **45**, 1311 (1980).
[5] N. Austern and C. M. Vincent, *Phys. Rev. C* **23**, 1847 (1981).
[6] X. H. Li, T. Udagawa, and T. Tamura, *Phys. Rev. C* **30**, 1895 (1984).
[7] T. Udagawa and T. Tamura, *Phys. Rev. C* **33**, 494 (1986).
[8] M. Ichimura, N. Austern, and C. M. Vincent, *Phys. Rev. C* **32**, 431 (1985).
[9] M. Ichimura, *Phys. Rev. C* **41**, 834 (1990).
[10] M. Hussein and K. McVoy, *Nucl. Phys. A* **445**, 124 (1985).
[11] M. S. Hussein and R. Mastroleo, *Nucl. Phys. A* **491**, 468 (1989).
[12] M. S. Hussein, T. Frederico, and R. Mastroleo, *Nucl. Phys. A* **511**, 269 (1990).
[13] J. Lei and A. Moro, *Phys. Rev. C* (to be published).
[14] B. V. Carlson, R. Capote, and M. Sin, [arXiv:1508.01466](https://arxiv.org/abs/1508.01466).
[15] T. Udagawa, Y. Lee, and T. Tamura, *Phys. Lett. B* **196**, 291 (1987).
[16] R. C. Mastroleo, T. Udagawa, and M. G. Mustafa, *Phys. Rev. C* **42**, 683 (1990).
[17] I. J. Thompson and F. M. Nunes, *Nuclear Reactions for Astrophysics* (Cambridge University Press, Cambridge, 2009).
[18] A. J. Koning and J. Delaroche, *Nucl. Phys. A* **713**, 231 (2003).
[19] C. Perey and F. G. Perey, *At. Data Nucl. Data Tables* **17**, 1 (1976).
[20] I. J. Thompson, *Comput. Phys. Rep.* **7**, 167 (1988).